Original Article

In Mice With Type 2 Diabetes, a Vascular Endothelial Growth Factor (VEGF)-Activating Transcription Factor Modulates VEGF Signaling and Induces Therapeutic Angiogenesis After Hindlimb Ischemia

Yongjun Li, Surovi Hazarika, Donghua Xie, Anne M. Pippen, Christopher D. Kontos, and Brian H. Annex

Peripheral arterial disease is a major complication of diabetes. The ability to promote therapeutic angiogenesis may be limited in diabetes. Type 2 diabetes was induced by high-fat feeding C57BL/6 mice (n = 60). Normal chow–fed mice (n = 20) had no diabetes. Mice underwent unilateral femoral artery ligation and excision. A plasmid DNA encoded an engineered transcription factor designed to increase vascular endothelial growth factor expression (ZFP-VEGF). On day 10 after the operation, the ischemic limbs received 125 μg ZFP-VEGF plasmid or control. Mice were killed 3, 10, or 20 days after injection (n = 10/group, at each time point). Limb blood flow was measured by laser Doppler perfusion imaging. VEGF mRNA expression was examined by real-time PCR. VEGF, Akt, and phospho-Akt protein were measured by enzyme-linked immunosorbent assay. Capillary density, proliferation, and apoptosis were assessed histologically. Compared with normal mice, mice with diabetes had greater VEGF protein, reduced phospho-Akt–to–Akt ratio before ligation, and an impaired perfusion recovery after ligation. At 3 and 10 days after injection, in mice with diabetes, gene transfer increased VEGF expression and signaling. At later time points, gene transfer resulted in better perfusion recovery. Gene transfer with ZFP-VEGF was able to promote therapeutic angiogenesis mice with type 2 diabetes. *Diabetes* 56:656–665, 2007

Peripheral arterial disease (PAD) is a major cause of morbidity and mortality in the U.S. (1). Type 2 diabetes is one of the strongest risk factors for the development of peripheral arterial obstructive disease (PAOD) (2,3). The two major clinical manifestations of PAD are intermittent claudication with leg pain or aching with exercise that is relieved with rest and critical limb ischemia with rest pain, ischemic ulcers, or gangrene (1). In many aspects, patients with PAD and diabetes have poorer clinical outcomes and poorer responses to pharmacological and revascularization therapies than patients with PAD without diabetes (2,4). Many patients with PAD and diabetes are not eligible or are poor candidates for revascularization, and there are currently no medical therapies available to improve perfusion and thereby alter the poor prognosis.

Angiogenesis is the growth and proliferation of new blood vessels from existing vascular structures (5). Therapeutic angiogenesis seeks to use this phenomenon for the treatment of disorders of inadequate tissue perfusion (6–8). The vascular endothelial growth factor (VEGF) family is perhaps the most extensively studied angiogenic growth factor (9). VEGF-A is known to be present in mammalian striated skeletal muscle and is transcribed as a single mRNA that undergoes differential splicing to result in expression of at least four splice variants ($VEGF_{121}$, $VEGF_{165}$, $VEGF_{189}$, and $VEGF_{206}$ in humans) that vary with respect to their solubility and binding to extracellular matrix proteoglycans (9,10). Expression of the different VEGF-A isoforms (hereafter referred to as VEGF) appears to be differentially regulated in the setting of ischemia (11). Preclinical models of PAOD have studied the effects of the delivery of a single isoform with different results (12,13). Placebo-controlled human trials performed to date have also tested effects of only a single isoform of VEGF, and the results of these trials have been disappointing (14,15).

One method to promote the production of multiple VEGF isoforms is by increasing endogenous VEGF gene transcription and subsequent protein expression. Previous data from our laboratory and others have demonstrated that delivery of an engineered zinc finger DNA protein linked to a transcriptional activator (called ZFP-VEGF) was able to increase endogenous VEGF expression in striated skeletal muscle and promote angiogenesis in both a mouse ear and rabbit hindlimb ischemia model (16,17). We recently demonstrated that after hindlimb ischemia, intramuscular delivery of a ZFP-VEGF was able to improve perfusion, limit tissue apoptosis, and promote angiogenesis in a ApoE knockout mice fed a high-cholesterol diet (7). Type 2 diabetes is associated with reduced VEGF signaling along with impaired angiogenesis and collateral

From the Division of Cardiology, Department of Medicine, Durham VA and Duke University Medical Center, Durham, North Carolina.

Address correspondence and reprint requests to Brian H. Annex, MD, Division of Cardiology, Durham Veterans Affairs and Duke University Medical Center, 508 Fulton St., Box 111A, Durham, NC 27710. E-mail: annex001@mc.duke.edu.

Received for publication 19 July 2006 and accepted in revised form 13 November 2006.

B.H.A.'s laboratory has received educational grants from Edwards Life Sciences, and B.H.A. has received consulting fees from Edwards Life Sciences.

Cox-2, cyclooxygenase 2; eNOS, endothelial NO synthase; iNOS, inducible NO synthase; PAD, peripheral arterial disease; PAOD, peripheral arterial obstructive disease; TUNEL, transferase-mediated dUTP nick-end labeling; VEGF, vascular endothelial growth factor; VEGFR, VEGF receptor.

DOI: 10.2337/db06-0999

blood vessel formation after ischemia; however, VEGF ligand availability may not be the limiting factor (13,18–20). Most preclinical models of PAD with diabetes use type 1 diabetes; thus, we sought to determine whether intramuscular delivery of the ZFP-VEGF plasmid could promote therapeutic angiogenesis in a mouse PAD model with type 2 diabetes.

RESEARCH DESIGN AND METHODS

Plasmid DNA constructs and formulations. The VEGF-activating ZFP was delivered via a previously described genetically engineered plasmid that encoded a three–zinc finger DNA-binding domain, the nuclear localization signal from simian virus 40 large T antigen, and the transactivation domain from the p65 subunit of the human nuclear factor-κB, subcloned into pVAX1 (Invitrogen, Carlsbad, CA) with expression under direction of the cytomegalovirus promoter (7,16). Controls in prior studies included the identical plasmid without the ZFP VEGF insert, β-galactosidase, and the presence or absence of poloxomer (7,17). Therefore, for this current study, vials containing poloxomer with and without plasmid were identical in appearance and were coded to maintain blinding until data analysis was complete.

Hindlimb ischemia models and treatment groups. In total, 60 male C57BL/6 mice (Jackson Laboratory, Bar Harbor, ME) at 4 weeks old were fed a high-fat diet to induce type 2 diabetes (21). In the high-fat diet (D12451; Research Diet, New Brunswick, NJ), 45% of total calories were from fat, which has been shown to induce obesity with increased insulin levels and insulin resistance in the absence of genetic mutations (22,23). After 12 weeks on the high-fat diet, glucose tolerance testing was performed in which mice were fasted overnight, provided water ad libitum, and given a glucose load of 1 mg/kg body wt by intraperitoneal injection. Blood glucose concentrations were measured before and 30, 60, and 90 min after, using a OneTouch Ultra glucometer (LifeScan, Milpitas, CA). Glucose tolerance was determined as the area under the curve of blood glucose concentrations. All high-fat diet–fed mice met the criteria for diabetes (23).

Mice were anesthetized by intraperitoneal injection of ketamine (90 mg/kg) and xylazine (10 mg/kg) and underwent surgically induced unilateral hindlimb ischemia with ligation and excision of the femoral artery from its origin just above the inguinal ligament to its bifurcation at the origin of the saphenous and popliteal arteries, using methods described previously (24). The inferior epigastric, lateral circumflex, and superficial epigastric artery branches were also isolated and ligated. Mice were closely monitored during the postoperative period and underwent laser Doppler perfusion imaging immediately after surgery and at 10-day intervals until the termination of the study. The extent of necrosis, if any, in ischemic hindlimbs was recorded one time between days 3 and 5 after surgery: grade 0, no necrosis in ischemic limb; grade I, necrosis limited to toes; grade II, necrosis extending to dorsum pedis; grade III, necrosis extending to crus; and grade IV, necrosis extending to thigh.

Ten days after the operation, the mice were anesthetized with 2% isoflurane (VETEQUIP inhalation anesthesia system; VETEQUIP, Pleasanton, CA), and hindlimb perfusion was recorded as the 0 time point. Mice were randomized in a blinded manner into either a ZFP-VEGF treatment group (125 μg ZFP-VEGF plasmid in 125 μl 1% poloxamer/50 mmol/l NaCl) or control, no ZFP-VEGF group (125 μl 1% Poloxamer/50 mmol/l NaCl). The dose and method of intramuscular injections were previously described (7). Group assignments were made to accomplish different study objectives. Based upon their group assignment, the study was completed 3, 10, or 20 days after injection.

Ten age-matched wild-type C57BL/6 mice fed normal chow were used as normal controls for body weights, glucose level, VEGF, phospho-Akt, Akt protein level, and capillary density in skeletal muscle. Another 10 mice fed normal chow underwent hindlimb ischemic surgery to get the comparable perfusion recovery data.

A single operator (Y.L.) blinded to group assignments performed all of the surgeries and treatments. All protocols and procedures involving animals conformed with the "Guidelines for Use of Laboratory Animals" published by the U.S. Department of Health and Human Services and were approved by the Duke University Animal Care and Use Committee. All animals received care in accordance with "Principles of Laboratory Animal Care," formulated by the National Society for Medical Research, and "Guide for the Care and Use of Laboratory Animals," published by the National Institutes of Health (NIH Publication No. 86-23, revised 1985).

Tissue harvest and preparation. Mice were anesthetized, underwent laser Doppler imaging, and were killed, as previously described (7). The distal portion of the ischemic and contralateral, nonischemic muscles was placed in 30% sucrose-PBS solution and mounted in cross section in OCT. Cryostat sections (5 μm) were prepared on microscope slides, and the remaining tissues were snap frozen in liquid N_2 for RNA and/or protein extraction.

Measurement of mRNA and protein. Total RNA was isolated and purified, and concentrations were determined by spectrophotometer, using methods previously described (7,17). For RT-PCR, primers, their sequences, and the amplifications conditions are shown in Table 1. Samples were subject to electrophoresis through an agarose gel, and water without primers served as the negative controls. For real-time PCR, 2 μg total RNA was used for first-strand cDNA synthesis by reverse transcription using SuperScript III First-Stand Synthesis System (Invitrogen), and 2 μl cDNA was quantitatively amplified using TaqMan Universal PCR Master Mix (AB Applied Biosystems, Foster City, CA). A single-tube PCR was optimized for the quantification of specific mouse primer and probe (Table 1) for VEGF. All real-time PCR data were measured and captured with a sequence detector, and mRNA concentrations were calculated using the *Ct* value representing the PCR cycle number at which fluorescence was detectable above an arbitrary threshold normalized against 18S rRNA, as previously described (17). Negative controls lacking cDNA were always included, and each sample was tested in triplicate.

Muscle samples were weighed, homogenized, centrifuged in Tris-saline buffer; protein concentrations were determined by Bradford assay; and total VEGF protein concentration was determined by a solid-state enzyme-linked immunoassay system, as previously described (17). Phospho-Akt and total Akt were measured using a Biosource AKT [pS473] and AKT ELISA kit, respectively (Invitrogen). Caspase activity was determined using Caspase-3 colorimetric assay kit (Biovision, Mountview, CA), and absorbance was normalized to the protein concentration in each sample. Data were expressed as units per milligrams of protein.

Electrophoresis and immunoblotting analysis. Protein samples were separated on SDS-polyacrylamide gels; transferred to a polyvinylidene difluoride membranes, which were treated with blocking buffer (5% skim milk); probed with a Ser473–phospho-Akt (1:1,000), Akt (1:1,000), anti–phospho–endothelial nitric oxide (NO) synthase (eNOS) Ser1177 (1:1,000), cyclooxygenase 2 (Cox-2) (1:500; Cell Signaling, Beverly, MA), or eNOS (1:1,000; Cell Signaling) antibodies overnight at 4°C; and then incubated with a horseradish peroxidase–conjugated anti-rabbit immunoglobulin (1:5,000; Cell Signaling) for 1 h at room temperature. Immune reactivity was visualized using ECL plus system. Quantification of results was performed by densitometry (ImageJ 1.36b; National Institutes of Health, Bethesda, MD) comparing the density of identically sized areas (corresponding to immunoreactive bands), and results were analyzed as total integrated density (arbitrary units).

Analysis of capillary density, proliferation, and apoptosis. Endothelial cells were identified by immunohistochemical staining using a rat anti-mouse CD31 antibody (1:200 dilution; Serotec, Raleigh, NC). Capillary density was measured by counting six random high-power (magnification ×200) fields or a minimum of 200 fibers from each ischemic and nonischemic limb on an inverted light microscope and was expressed by the number of $CD31^+$ cells per square millimeter or per fiber. Area was measured with an NIH Image analysis system.

Cell proliferation and apoptosis in skeletal muscle was detected with immunohistochemical staining of proliferating cell nuclear antigen (PCNA, 1:50 dilution; Santa Cruz Biotechnology, Santa Cruz, CA) and transferase-mediated dUTP nick-end labeling (TUNEL) staining (ApopTag *In Situ* kit; Chemicon, Temecula, CA), respectively. The proliferation index and apoptotic index were expressed by the percentage of the number of positive nuclei divided by the total number of counted nuclei. The count was performed on three randomly selected fields (magnification ×200) and at least 200 nuclei per sample. A single reader (K.W. [see ACKNOWLEDGMENTS]) blinded to the sample type performed all the analysis.

Hemodynamic assessment. Bilateral hindlimb perfusion was measured using a Laser Doppler Perfusion Imager system (PERIMED, Stockholm, Sweden). Briefly, mice received anesthesia with 2% isoflurane, and hair was removed from both legs using a depilatory cream, whereas mice were maintained on a heating plate to minimize temperature variations. The laser Doppler perfusion imager used a beam from a 2-mW helium-neon laser that sequentially scanned a 12- × 12-cm tissue surface to a depth of a few hundred microns. During the scanning procedure, the moving blood cells shifted the frequency of incident light according to the Doppler principle. The backscattered light was collected by a photodiode collector, transformed into voltage variations, and expressed as a color-coded image representing the microvascular blood flow distribution. The results at any time point were expressed as a ratio of perfusion in the left (ischemic) versus right (normal) limb. Changes in perfusion were calculated as the ratio at the final time minus the baseline ratio, and this baseline (or day 0 value) was the immediate after-ligation value for the comparison of the mice with diabetes versus without diabetes and was the preinjection value for the effect of ZFP-VEGF treatment versus control over time.

TABLE 1
Primers and probes for real-time PCR and RT-PCR

Primer and probe	Sequences 5′-3′	PCR
Mouse VEGF		Real-time PCR
Forward primer	TACTGCTGTACCTCCACCTCCACCATG	
Reverse primer	TCACTTCATGGGACTTCTGCTCT	
Probe	AAGTGGTCCCAGGCTGCACCCAC	
Mouse 18S RNA		Real-time PCR
Forward primer	CGGCTACCACATCCAAGGAA	
Reverse primer	AGCCGCGGTAATTCCAGC	
Probe	TGCTGGCACCAGACTTGCCCTC	
Mouse VEGF A		Reverse transcriptase conditions
Forward primer	CTGTGCAGGCTGCTGTAACG	
Reverse primer	GTTCCCGAAACCCTGAGGAG	
Mouse VEGF B		Denaturation, 94°C for 30; annealing, 56°C for 30 s; elongation, 72°C for 1 min; 30 cycles
Forward primer	GATCCAGTACCCGAGCAGTC	
Reverse primer	GCACCTACAGGTGTCTGGGT	
Mouse VEGF C		
Forward primer	CAAGGCTTTTGAAGGCAAAG	
Reverse primer	TGCTGAGGTAACCTGTGCTG	
Mouse VEGF D		
Forward primer	CTCCAGGAACCCACTCTCTG	
Reverse primer	TCCTGGCTGTAGAGTCCCTG	
Mouse VEGF R1		Denaturation, 94°C for 30 s; annealing, 58°C for 30 s; elongation, 72°C for 1 min; 30 cycles
Forward primer	GTCACAGATGTGCCGAATGG	
Reverse primer	TGAGCGTGATCAGCTCCAGG	
Mouse VEGF R2		
Forward primer	AGAACACCAAAAGAGAGAGGAACG	
Reverse primer	GCACACAGGCAGAAACCAGTAG	

Statistical analysis. Results are expressed as means ± SE. For comparison of mean data on ZFP-VEGF treatment versus control, at one time point (i.e., VEGF expression, phospho-Akt–to–Akt ratio, vascular density, proliferation, and apoptosis index), statistical significance was evaluated by use of two-tailed Student's paired *t* test. To determine the effect of ZFP-VEGF treatment versus control on the change in perfusion ratio over time, a standard variance ANOVA repeated measure was performed. *P* values <0.05 were considered to be significant.

RESULTS

Mice with type 2 diabetes have impaired perfusion recovery after hindlimb ischemia. After 12 weeks of high-fat diet, C57BL/6 mice ($n = 60$) developed type 2 diabetes. Compared with age-matched normal chow–fed mice ($n = 10$), those with diabetes had significantly greater body weight (34.63 ± 4.67 vs. 26.18 ± 1.27 g; $P < 0.05$), fasting glucose levels (124.6 ± 29.3 vs. 92.6 ± 11.3 mg/dl; $P < 0.001$), and impaired glucose tolerance (22,585 ± 561 vs. 14,811 ± 541 $mg \cdot dl^{-1} \cdot min^{-1}$; $P < 0.001$) (22).

Age- and sex-matched mice with and without diabetes ($n = 10$ per group) underwent surgically induced hindlimb ischemia. Although both groups demonstrated increases in the perfusion ratio over time (Fig. 1*A*), the recovery was significantly blunted in the mice with diabetes. The magnitude of the change in the perfusion ratio was assessed by subtracting the day-10, -20, or -30 perfusion ratio from the ratio immediately after ligation (day 0), and this change in perfusion was different between mice with type 2 diabetes and control at the day-10 (0.24 ± 0.07 vs. 0.35 ± 0.02; $P < 0.05$), day-20 (0.34 ± 0.07 vs. 0.53 ± 0.08; $P < 0.05$), and day-30 (0.33 ± 0.04 vs. 0.58 ± 0.02; $P < 0.001$) time points. A sizeable fraction (35%) of mice with type 2 diabetes showed evidence of grade I (28.33%), II (5.0%), or III (1.67%) limb necrosis, whereas necrosis was not evident in any control mice.

In the absence of ischemia, as shown in Fig. 1*B*, capillary density in the gastrocnemius muscle was similar between mice with type 2 diabetes versus mice without diabetes (433 ± 30/area vs. 435 ± 35/area, or 1.31 ± 0.04/fiber vs. 1.46 ± 0.08/fiber; NS). Although VEGF protein expression (Fig. 1*B*, *right*) was significantly greater (26.27 ± 1.16 vs. 22.69 ± 0.93 pg/mg; $P < 0.05$), the ratio of phospho-Akt to total Akt (Fig. 1*C*) was lower (0.38 ± 0.08 vs. 0.76 ± 0.13; $P < 0.05$).

ZFP-VEGF gene transfer increases VEGF mRNA, protein, and signaling in ischemic muscle of mice with diabetes. Mice with type 2 diabetes were randomly assigned to receive either ZFP-VEGF plasmid or control ($n = 10$/group) injections into the ischemic hindlimb muscle 10 days after ischemia. Expression of VEGF mRNA, protein, and signaling ($n = 6$) was measured 3 days later. VEGF mRNA and protein levels were expressed as the copies of mRNA or concentration of protein in the ischemic gastronomes muscle minus the nonischemic muscle, for each mouse. As shown in Fig. 2*A*, VEGF mRNA copy number was significantly greater in the ZFP-VEGF treatment versus control (7.23 ± 2.60 vs. −0.89 ± 0.24; $P < 0.05$). Similarly, VEGF protein expression was significantly greater in the ZFP-VEGF treatment versus control (9.50 ± 3.53 vs. −3.95 ± 1.26 pg/mg; $P < 0.05$). By Western blotting (Fig. 2*B*, *left*), phospho-Akt was higher in ZFP-VEGF treatment compared with control. Quantitative ELISA assay showed that the phospho-Akt–to–Akt ratio (Fig. 2*B*, *right*) was significantly greater with ZFP-VEGF versus control treatment (0.74 ± 0.03 vs. 0.51 ± 0.15; $P < 0.05$). Finally, Fig. 2*C*, *left*, showed that more phosphorylated

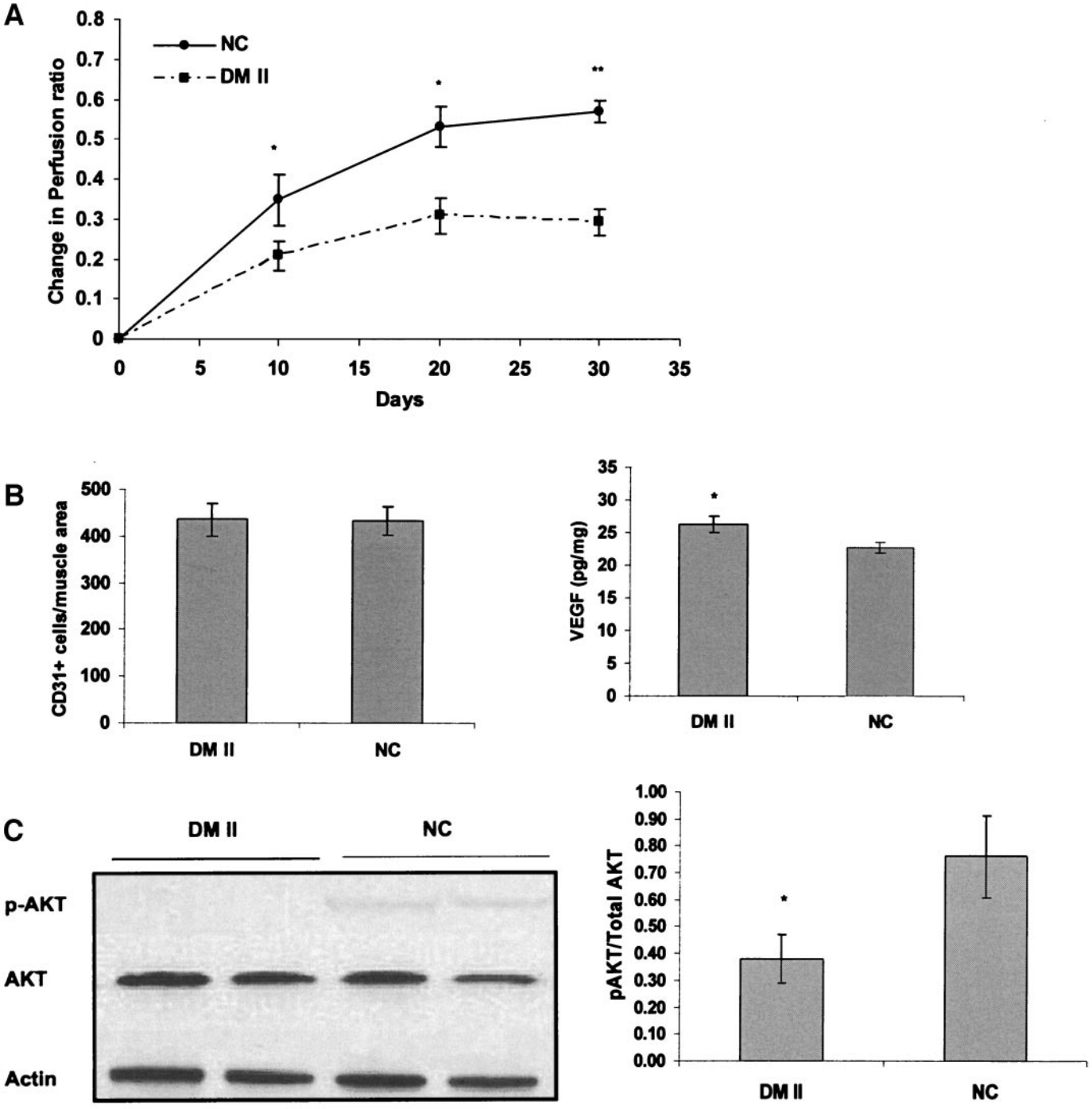

FIG. 1. ***A*****: Mice with type 2 diabetes (DM II, $n = 10$) had impaired perfusion recovery compared with mice fed normal chow (NC) and nondiabetic mice ($n = 10$). Graphs show the change in the perfusion ratio that is obtained by taking the perfusion ratio at follow-up minus the value of the perfusion ratio obtained immediately after surgery. The differences in perfusion recovery were significant at all time points. *$P < 0.05$; **$P < 0.001$. *B*: There was no difference in capillary density (*left*) in the nonischemic gastrocnemius muscle, between mice with diabetes versus normal chow (NC, $n = 10$/group). VEGF protein (*right*) in normal gastrocnemius was higher in mice with diabetes ($n = 10$) than normal chow–fed mice ($n = 10$) (26.27 ± 1.16 vs. 22.69 ± 0.93 pg/mg; *$P < 0.05$). *C*: Western blot (*left*) shows lower phospho-Akt–to–Akt ratio in mice with diabetes compared with normal chow ($n = 4$/group) and quantitative results (*right*) from density scanning was 0.38 ± 0.08 vs. 0.76 ± 0.13; *$P < 0.05$.**

eNOS was present in ZFP-VEGF treatment compared with the control. Quantitative analysis with Image J showed that the phospho-eNOS–to–eNOS ratio was significant increase with ZFP-VEGF versus control treatment, 0.83 ± 0.06 vs. 0.48 ± 0.11; $P < 0.05$ (integrated density, Fig. 2*C*, *right*). By PCR, VEGF-A was greater in ZFP-VEGF versus control treatment, but there were no differences in VEGF-B, VEGF-C, VEGF-D, or VEGF receptor (VEGFR) 1 or 2 (Fig. 3*A* and *B*). To exclude differences in the inflammatory response, inducible NO synthase (iNOS) mRNA was similar with ZFP-VEGF or control treatment (Fig. 3*C*).

Next, 20 mice were randomly assigned to receive either ZFP-VEGF plasmid or control ($n = 10$/group) injection into the gastrocnemius muscle 10 days after hindlimb ischemia are harvested 10 days after gene transfer (20 days

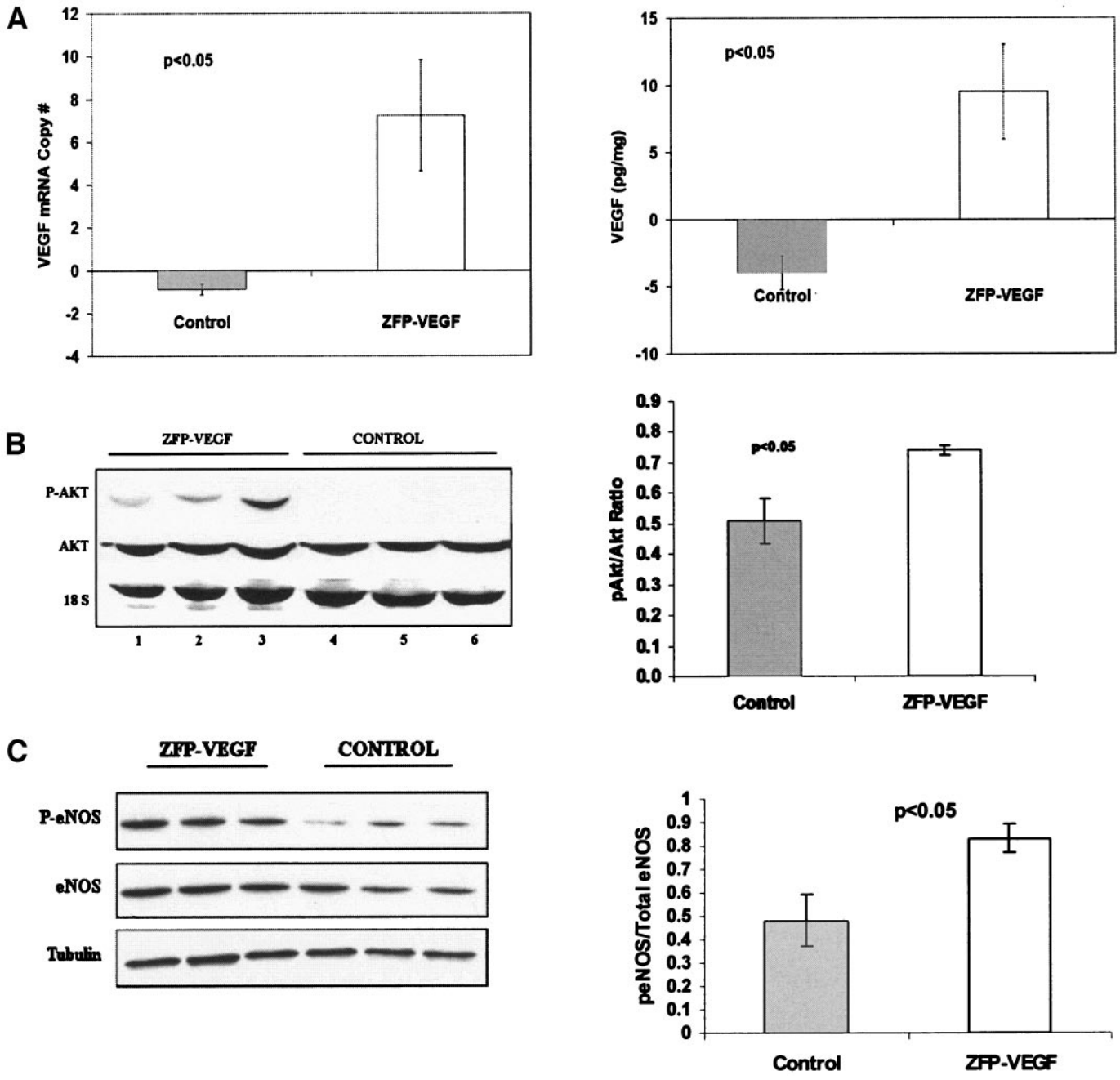

FIG. 2. Three days after gene transfer, ZFP-VEGF plasmid in poloxomer treatment increased the expression of VEGF mRNA, VEGF protein, phospho-Akt, and phospho-eNOS expression in ischemic skeletal muscle compared with control (poloxomer only) injection. *A*: VEGF mRNA (*left*) and protein (*right*) was expressed as the copies of mRNA or concentration of protein in the ischemic minus the nonischemic limb, for each mouse. VEGF mRNA was greater with *ZFP-VEGF* versus control treatment (n = 6/group). VEGF protein was greater with *ZFP-VEGF* versus control treatment (n = 4/group). *B*: Western blot showed more phospho-Akt with *ZFP-VEGF* (*lanes 1–3*) versus control (*lanes 4–6*) treatment. By ELISA, there was an increase in phospho-Akt/Akt in *ZFP-VEGF* versus control treatment (n = 4/group; $P < 0.05$). *C*: Western blot also showed more phosphorylated eNOS (P-eNOS) with *ZFP-VEGF* versus control treatment (n = 3/group), and the results were quantified by integrated density (*right*; $P < 0.05$).

after hindlimb ischemia). Expression of VEGF protein (n = 8) and signaling (n = 7) were assessed as above. As shown in Fig. 4*A*, VEGF protein expression was significantly greater in the ZFP-VEGF treatment versus control treatment (6.57 ± 1.58 vs. −1.63 ± 2.3 pg/mg; $P < 0.05$). By ELISA, the phospho-Akt–to–Akt ratio (Fig. 4*B*) was significantly greater with ZFP-VEGF treatment, 0.56 ± 0.08 vs. 0.39 ± 0.07; $P < 0.05$. Although changes in the perfusion ratio (0.10 ± 0.03 vs. 0.069 ± 0.03; NS) were similar in the ZFP-VEGF treatment versus control (n = 10 for each), as shown in Fig. 5*A*, capsize activity was lower in the ZFP-VEGF treatment versus control treatment 0.06 ± 0.01 vs. 0.16 ± 0.04; $P < 0.05$ (n = 6/group). Although VEGFR1 and -2 mRNA levels were similar at 3 days after gene transfer in the ischemic gastrocnemius muscle, as shown in Fig. 5*B*, VEGF R1 was lower in the ZFP-VEGF versus control treatment with no difference in VEGF R2. Finally, as shown in Fig. 5*C*, protein levels of the inflammatory marker Cox-2 was similar between ZFP-VEGF treatment versus control.

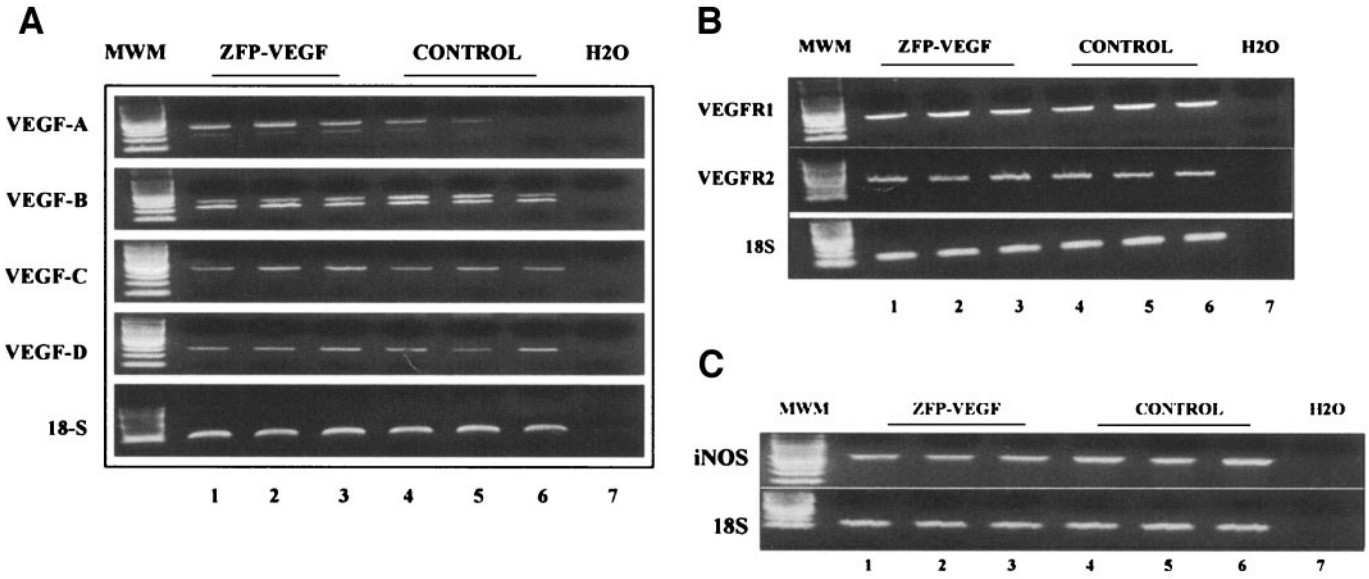

FIG. 3. PCR of mRNA isolated from ischemic gastrocnemius muscle 3 days after gene transfer, *ZFP-VEGF* plasmid compared with control. *A* and *B*: The primers and conditions are shown in Table 1. *A*: VEGF-A mRNA is increased with *ZFP-VEGF* (*lanes 1–3*) versus control treatment (*lanes 4–6*), whereas VEGF-B, VEGF-C, and VEGF-D are unchanged. Molecular weight marker (MWM) and H_2O (*lane 7*) served as the negative control. *B*: VEGFR1 and VEGFR2 were similar between ZFP-VEGF (*lanes 1–3*) versus control treatment (*lanes 4–6*). *C*: iNOS mRNA was similar between ZFP-VEGF (*lanes 1–3*) versus control treatment (*lanes 4–7*), and for iNOS, the primers were 3′-5′ CAGGACCACACCCCCTCGGA and 5′-3′ AGCCACATCCCGAGCCATGC with denaturation at 94°C for 35 s, annealing 65°C for 1 min, and extension at 72°C for 1 min.

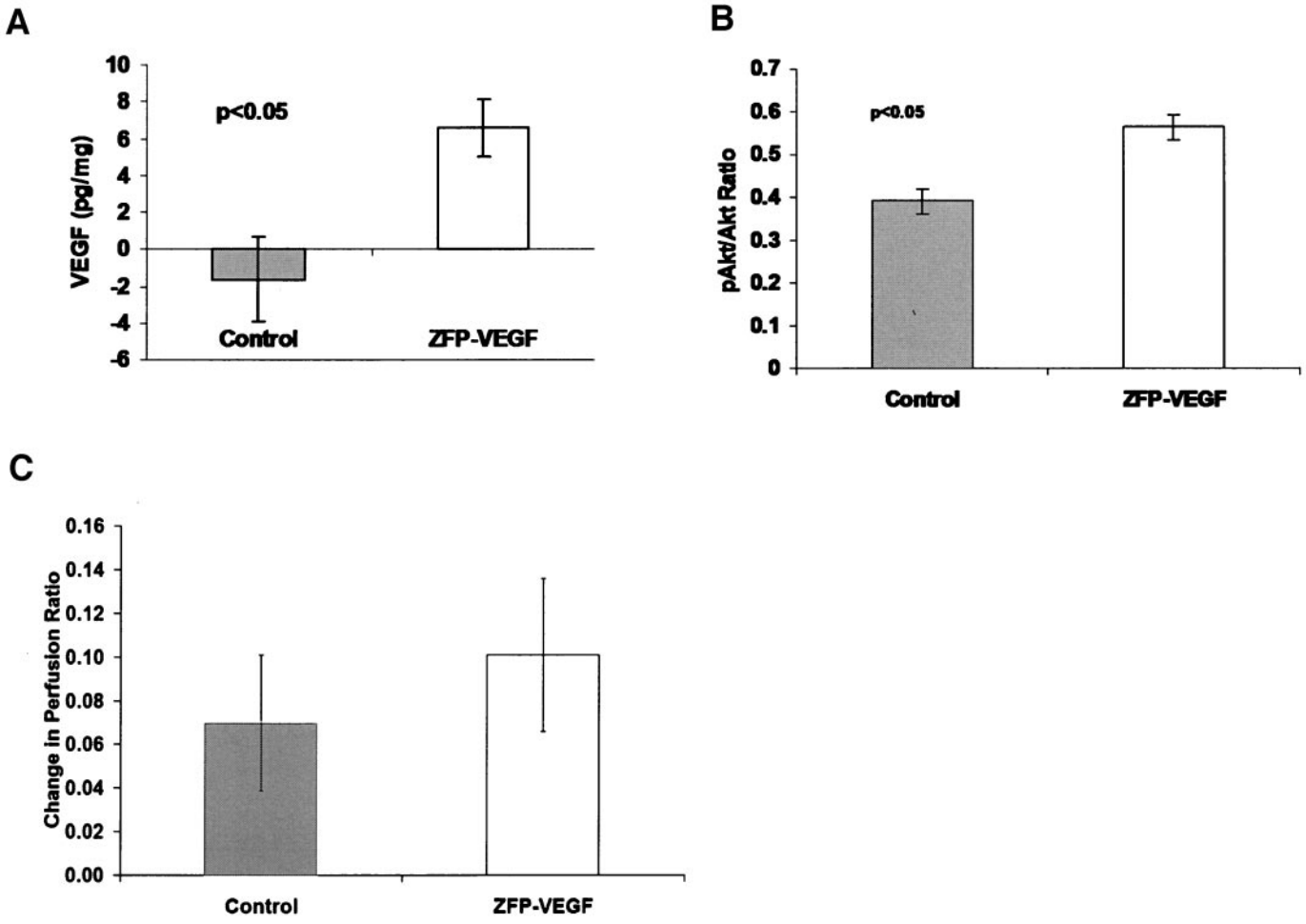

FIG. 4. Ten days after gene transfer, treatment with ZFP-VEGF plasmid increased VEGF protein and phospho-Akt–to–Akt ratio in ischemic skeletal muscle compared with control treatment, with no change in perfusion recovery. *A*: VEGF protein (*right*) was calculated as in Fig. 2 and, VEGF protein was greater with ZFP-VEGF versus control treatment (n = 8/group). *B*: The phospho-Akt–to–Akt ratio was calculated from ELISA data and was significantly greater in ZFP-VEGF versus control treatment (n = 7/group). *C*: The change in the perfusion ratio was calculated from preinjection to day 10 was not different in the ZFP-VEGF versus control treatment (n = 10/group).

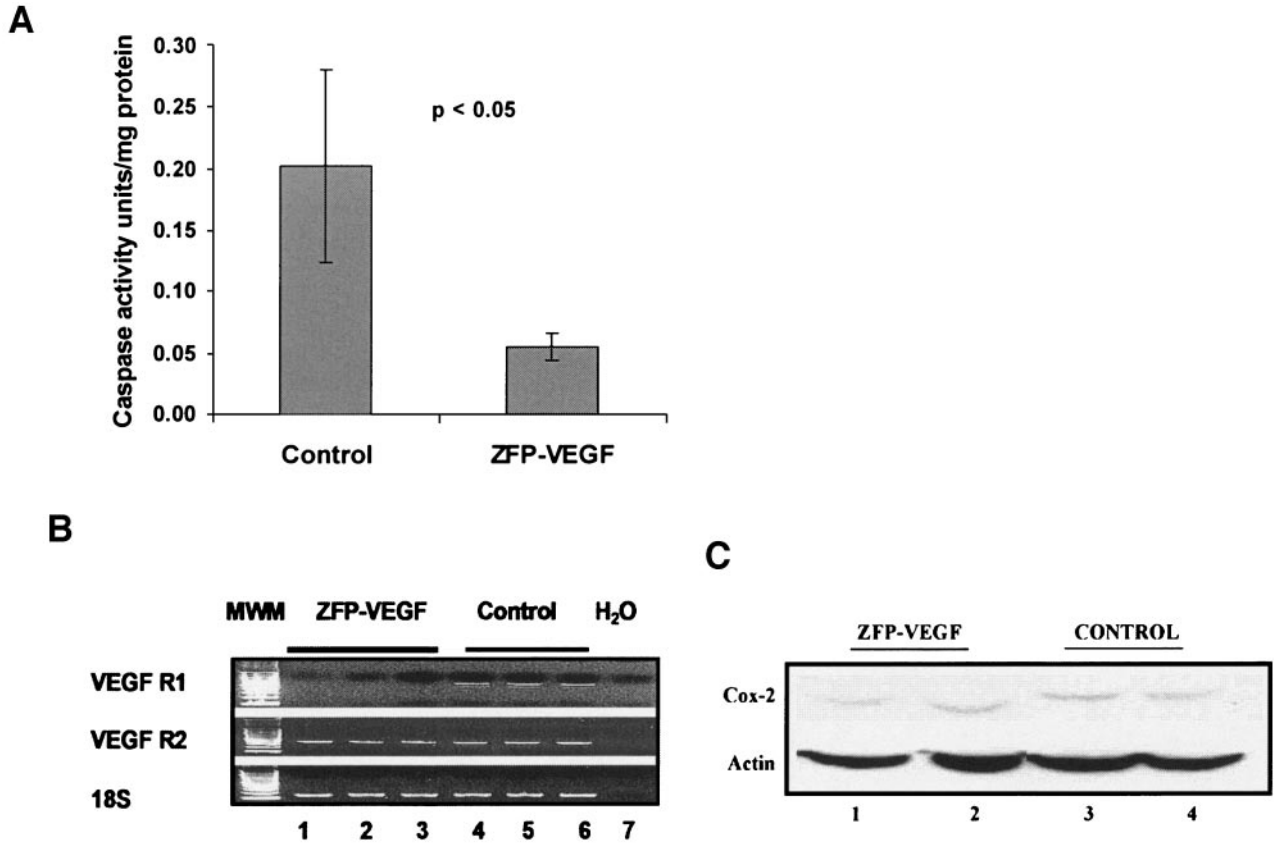

FIG. 5. Ten days after gene transfer, treatment with ZFP-VEGF plasmid resulted in changes in caspase activity and VEGFR mRNA with no change in cycloxygenase-2 expression in ischemic skeletal muscle compared with control treatment. *A*: Caspase activity was significantly lower in ZFP-VEGF versus control treatment (n = 6/group; $P < 0.05$). Caspase activity was expressed as units per milligram soluble protein. *B*: VEGFR1 was lower between ZFP-VEGF (*lanes 1–3*) versus control treatment (*lanes 4–6*), whereas VEGFR2 was unchanged. As in Fig. 3, molecular weight marker (MWM) and H_2O (*lane 7*) served as a negative control. *C*: Cox-2 protein was similar between ZFP-VEGF (*lanes 1* and *2*) versus control treatment (*lanes 3* and *4*).

ZFP-VEGF treatment results in improved in perfusion and favorably modulates capillary density, cell proliferation, and apoptosis in ischemic skeletal muscle of diabetic mice. Twenty mice were randomly assigned to receive either ZFP-VEGF plasmid or control (n = 10/group) injection into the ischemic gastrocnemius muscle 10 days after hindlimb ischemia. Laser Doppler perfusion imaging was performed before and at 10-day intervals after gene transfer. Before gene transfer, the perfusion ratio was similar between the ZFP-VEGF–treated and control-treated groups (0.62 ± 0.03 vs. 0.65 ± 0.03). By ANOVA, there was perfusion recovery over time in both the ZFP-VEGF and the control treatment groups. As we observed before (prior paragraph), there was a trend toward an increase in perfusion ratio in ZFP-VEGF versus control treatment (0.162 ± 0.022 vs. 0.103 ± 0.023; P = 0.08) at 10 days after injection (Fig. 6*A*). At 20 days after gene transfer, there was a clear and statistically significant increase in the change in the perfusion ratio with ZFP-VEGF treatment (0.241 ± 0.021 vs. 0.086 ± 0.016; $P <$ 0.001, Fig. 6*A*).

Capillary density (Fig. 6*B*) in the ischemic gastrocnemius muscle was significantly higher in the ZFP-VEGF versus control-treated mice (528 ± 29 vs. 444 ± 17; $P <$ 0.01). To exclude any potential differences induced by muscle edema or atrophy, the capillary–to–muscle fiber ratio in the ischemic muscle was also measured. Like capillary density, the capillary–to–muscle fiber ratio was significantly higher in the ZFP-VEGF versus control-treated mice (1.51 ± 0.06 vs. 1.28 ± 0.05; $P < 0.01$). The fraction of PCNA-positive cells (Fig. 6*B*) in the ischemic gastrocnemius muscle was significantly greater in ZFP-VEGF versus control-treated mice (2.56 ± 0.37 vs. 0.76 ± 0.28%; $P < 0.01$). Apoptosis as measured by TUNEL-positive nuclei in the ischemic muscle (Fig. 6*B*) was significantly decreased in ischemic muscle of ZFP-VEGF versus control-treated mice (1.50 ± 0.21 vs. 2.25 ± 0.25%; $P < 0.05$).

DISCUSSION

Type 2 diabetes is a major risk factor for the development of PAOD (2,3). When diabetes is superimposed on PAD, there is a poorer clinical prognosis, and surgical and/or catheter-based revascularization frequently cannot be used in a sizable fraction of these patients. Therefore, therapeutic angiogenesis is being actively explored as a future treatment for patients with PAD, many of whom will have superimposed type 2 diabetes (5,7,8). To the best of our knowledge, this report is the first to investigate the therapeutic efficiency of VEGF in a preclinical PAD model with diet-induced type 2 diabetes. The major findings of our study were that diet-induced diabetes was associated with: *1*) an impaired perfusion recovery after hindlimb ischemia; *2*) an increase in VEGF ligand but reduced VEGF signaling in skeletal muscle in the absence of ischemia; and *3*) gene transfer with a transcription factor designed to increase VEGF expression into an ischemic

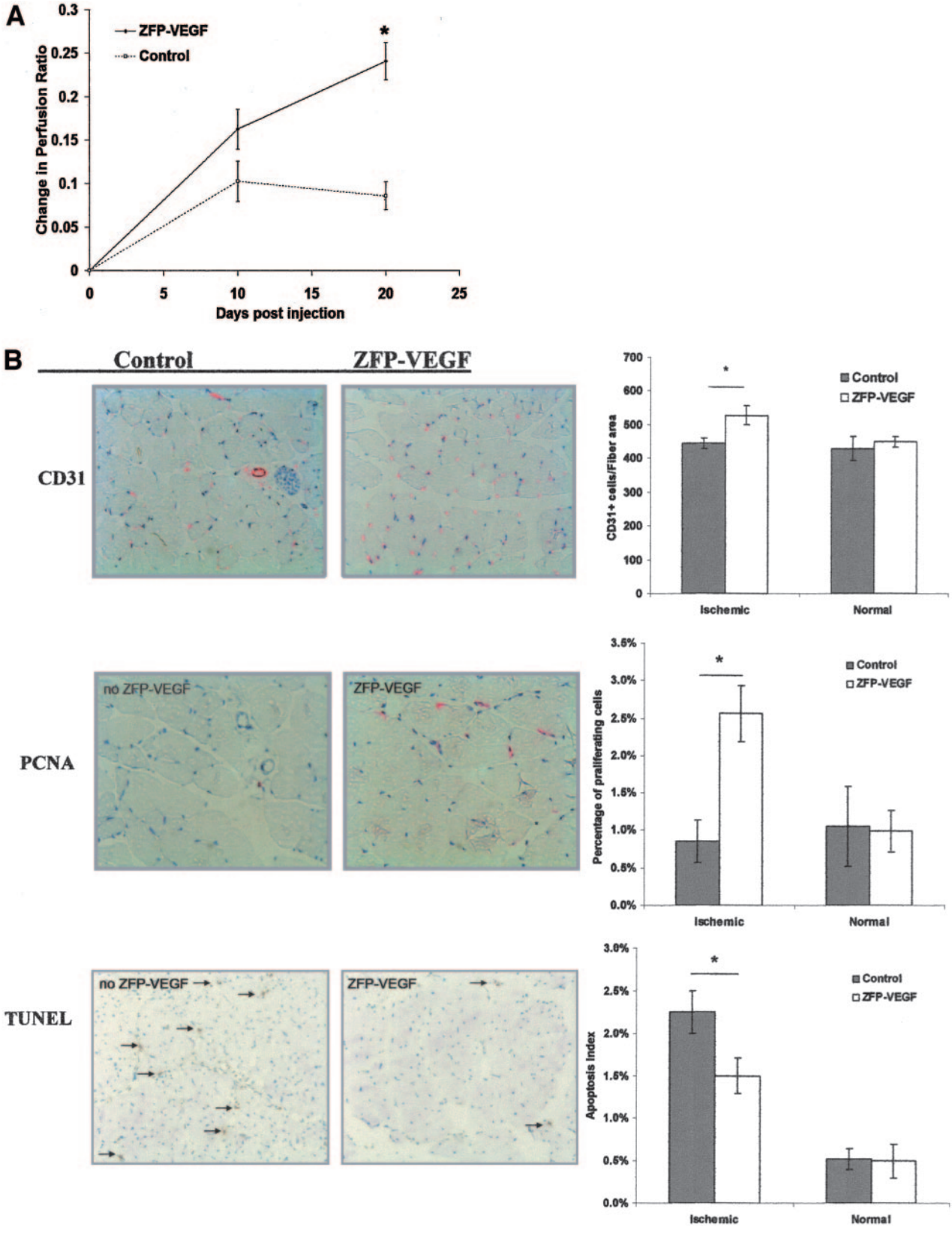

FIG. 6. By 20 days after gene transfer, ZFP-VEGF versus control treatment was associated with improved perfusion to the ischemic limb and differences in capillary density, proliferation, and apoptosis in ischemic gastrocnemius muscle. *A*: Changes in the perfusion ratio were calculated as the perfusion ratio at follow-up minus the ratio preinjection (labeled day 0). There was no difference on day 10 with ZFP-VEGF versus control treatment (n = 10/group); however, the difference was significant on day 20 after injection, *P < 0.001. *B*: *Top*, a representative CD31 immunohistochemistry staining for capillary density; red dots indicate capillaries (magnification ×200). *Middle*, PCNA staining; red dots represent proliferating cells. *Bottom*, TUNEL staining for apoptosis; brown dots indicate apoptotic cells (magnification ×100). Graphs to the right of photographs represent the quantitative assessments with n = 10/group for all comparisons. Capillary density was increased with ZFP-VEGF versus control treatment, *P < 0.01. Proliferation cells were greater with ZFP-VEGF versus control treatment, *P < 0.01. Apoptosis index was lower with ZFP-VEGF versus control treatment, *P < 0.05.

limb, increase VEGF signaling, and improve the perfusion recovery.

A VEGF signaling defect may be one of the reasons for the reduced collateral blood vessel growth seen in patients with diabetes (18–20,25). Sasso et al. (19) showed that patients with diabetes had reduced VEGF signaling in the myocardium despite an increase in VEGF ligand (19). We found greater levels of the VEGF ligand with reduced VEGF signaling in hindlimb muscle before ligation, and after ligation this was associated with an impaired perfusion recovery by laser Doppler and a greater extent of tissue necrosis. Despite an increase in ligand levels, we found that this transcription factor was able to further increase VEGF ligand expression and substantially correct the VEGF signaling defect in ischemic muscle in the early days after gene transfer in mice with diabetes. Akt is a serine/threonine protein kinase and is activated by phosphorylation from phosphoinositide-dependent kinases, and the phosphorylation of eNOS is one of the targets of phospho-Akt (26,27). The correction in VEGF signaling was followed by improvements in tissue perfusion, greater amounts of cell proliferation, and reduced apoptosis in the treated limb. Interestingly, in a rat model of streptozotocin-induced type 1 diabetes, the delivery of an engineered VEGF transcription factor was protective against diabetic neuropathy, and the authors also demonstrated that conditioned medium from transfected cells protected human neuroblastoma cells from serum starvation, indicating a direct cytoprotective effect (16). Take together these data suggest that modulating VEGF expression remains an option as a therapeutic target even in the setting of type 2 diabetes.

Ischemic injury is a potent stimulus for increasing VEGF and inflammation before initiating angiogenesis (28). However, in current study, we found an attenuated increase in VEGF after ischemic injury in mice with type 2 diabetes at both days 13 and 20 after ligation, as shown by a negative value when VEGF expression was compared with the opposite limb (Figs. 2*A* and 4*A*). This finding was consistent with the findings of Schiekofer et al. (29) who used Lepr$^{db/db}$ mice and microarrays to identify hindlimb cDNA expression profiles before and after ischemia. Unlike the wild-type mice, VEGF-A was not upregulated in Lepr$^{db/db}$ mice on days 1, 7, or 14 after surgery. The NOD model is characterized by a leukocytic infiltration of the pancreatic islets and immune dysfunctions (30). Rivard et al. (12) in NOD mice reported lower VEGF expression in ischemic muscle compared with wild-type mice from days 3 to 14 after surgery, even when glucose was controlled with insulin. They reported an impairment of perfusion recovery and neo-capillary formation in the NOD versus wild-type mice that was corrected with adeno-VEGF (murine VEGF$_{164}$) delivered immediately after surgery. Although in our study we showed an increase in VEGF expression after gene transfer, we did not find differences in iNOS or Cox-2 in the ZFP-VEGF versus control-treated muscle to implicate alterations in inflammation. Although poloxomer was present in our study, it was present in both groups, and prior studies from our laboratory did not find that the presence or absence of poloxomer was associated with differences in VEGF expression (7,17) or cellular infiltration (7).

VEGF has several isoforms that arise from differential splicing that are differentially regulated in the setting of ischemia. In mice with streptozotocin-induced type 1 diabetes, Roguin et al. (13) found no benefit on perfusion flow restoration from a continually delivery of rat VEGF-165 plasmid (90% homology of mouse VEGF) into ischemic muscle, although they did find an apparent increase in factor VIII–positive cells and smooth muscle actin–positive cells in the ischemic muscle of diabetic mice that received VEGF. Data from placebo-controlled human clinical trials have not been encouraging (14,15). Modulating endogenous VEGF transcription is one method to alter multiple VEGF isoforms, and we found that the ZFP-VEGF–activating transcription factor could upregulate VEGF-A in ischemic muscle from mice with diabetes. Interestingly, at 3 days after gene transfer, there was no difference in VEGF-B, VEGF-C, VEGF-D, and VEGFR1 or -2 in muscle treated with the ZFP-VEGF compared with control. At a later time point, we found more VEGFR2 relative to VEGFR1 mRNA. Studies from knockout mice have shown that VEGFR2 is an angiogenic VEGFR, and VEGFR1 may actually have an inhibitory role. Whereas VEGFR2-deficient mice die because of a failure to develop blood vessels or even endothelial cells at all, VEGFR1-deficient mice appear to have an overgrowth of endothelial cells that fail to properly pattern into normal vessels (31,32). These data suggested that a role of VEGFR1 is to limit endothelial cell proliferation. Further studies have shown that VEGFR1 limits VEGFR2-mediated endothelial cell proliferation through a pathway involving VEGFR1-mediated activation of phosphoinositide 3-kinase and subsequent NO production. (33,34). Whether modulating multiple VEGF isoforms will lead to better efficacy in humans compared with single isoform therapy remains to be determined.

ACKNOWLEDGMENTS

This study was supported by the Iacoccoa Foundation. The ZFP-VEGF plasmid in poloxomer and the poloxomer control vials were provided by Edwards Life Sciences.

We acknowledge Shelley Odronic, Erika Reed, Karen Wu, and Conrad Ireland for their assistance. We thank Shoukang Zhu from Dr. Pascal Goldschmidt's laboratory for help in the real-time PCR studies.

REFERENCES

1. Ouriel K: Peripheral arterial disease. *Lancet* 358:1257–1264, 2001
2. Beckman JA, Creager MA, Libby P: Diabetes and atherosclerosis: epidemiology, pathophysiology, and management. *JAMA* 287:2570–2581, 2002
3. Grundy SM, Benjamin IJ, Burke GL, Chait A, Eckel RH, Howard BV, Mitch W, Smith SC Jr, Sowers JR: Diabetes and cardiovascular disease: a statement for healthcare professionals from the American Heart Association. *Circulation* 100:1134–1146, 1999
4. Renard CB, Kramer F, Johansson F, Lamharzi N, Tannock LR, von Herrath MG, Chait A, Bornfeldt KE: Diabetes and diabetes-associated lipid abnormalities have distinct effects on initiation and progression of atherosclerotic lesions. *J Clin Invest* 114:659–668, 2004
5. Folkman J: Seminars in medicine of the Beth Israel Hospital, Boston: clinical applications of research on angiogenesis. *N Engl J Med* 333:1757–1763, 1995
6. Isner JM: Therapeutic angiogenesis: a new frontier for vascular therapy. *Vasc Med* 1:79–87, 1996
7. Xie D, Li Y, Reed EA, Odronic SI, Kontos CD, Annex BH: An engineered vascular endothelial growth factor-activating transcription factor induces therapeutic angiogenesis in ApoE knockout mice with hindlimb ischemia. *J Vasc Surg* 44:165–175, 2006
8. Simons M: Angiogenesis: where do we stand now? *Circulation* 111:1556–1566, 2005
9. Ferrara N, Davis-Smyth T: The biology of vascular endothelial growth factor. *Endocr Rev* 18:4–25, 1997
10. Robinson CJ, Stringer SE: The splice variants of vascular endothelial growth factor (VEGF) and their receptors. *J Cell Sci* 114:853–865, 2001
11. Cherwek DH, Hopkins MB, Thompson MJ, Annex BH, Taylor DA: Fiber

type-specific differential expression of angiogenic factors in response to chronic hindlimb ischemia. *Am J Physiol Heart Circ Physiol* 279:H932–H938, 2000
12. Rivard A, Silver M, Chen D, Kearney M, Magner M, Annex B, Peters K, Isner JM: Rescue of diabetes-related impairment of angiogenesis by intramuscular gene therapy with adeno-VEGF. *Am J Pathol* 154:355–363, 1999
13. Roguin A, Nitecki S, Rubinstein I, Nevo E, Avivi A, Levy NS, Abassi ZA, Sabo E, Lache O, Frank M, Hoffman A, Levy AP: Vascular endothelial growth factor (VEGF) fails to improve blood flow and to promote collateralization in a diabetic mouse ischemic hindlimb model. *Cardiovasc Diabetol* 2:18, 2003
14. Rajagopalan S, Mohler ER III, Lederman RJ, Mendelsohn FO, Saucedo JF, Goldman CK, Blebea J, Macko J, Kessler PD, Rasmussen HS, Annex BH: Regional angiogenesis with vascular endothelial growth factor in peripheral arterial disease: a phase II randomized, double-blind, controlled study of adenoviral delivery of vascular endothelial growth factor 121 in patients with disabling intermittent claudication. *Circulation* 108:1933–1938, 2003
15. Henry TD, Annex BH, McKendall GR, Azrin MA, Lopez JJ, Giordano FJ, Shah PK, Willerson JT, Benza RL, Berman DS, Gibson CM, Bajamonde A, Rundle AC, Fine J, McCluskey ER: The VIVA trial: vascular endothelial growth factor in ischemia for vascular angiogenesis. *Circulation* 107: 1359–1365, 2003
16. Price SA, Dent C, Duran-Jimenez B, Liang Y, Zhang L, Rebar EJ, Case CC, Gregory PD, Martin TJ, Spratt SK, Tomlinson DR: Gene transfer of an engineered transcription factor promoting expression of VEGF-A protects against experimental diabetic neuropathy. *Diabetes* 55:1847–1854, 2006
17. Dai Q, Huang J, Klitzman B, Dong C, Goldschmidt-Clermont PJ, March KL, Rokovich J, Johnstone B, Rebar EJ, Spratt SK, Case CC, Kontos CD, Annex BH: Engineered zinc finger-activating vascular endothelial growth factor transcription factor plasmid DNA induces therapeutic angiogenesis in rabbits with hindlimb ischemia. *Circulation* 110:2467–2475, 2004
18. Simons M: Angiogenesis, arteriogenesis, and diabetes: paradigm reassessed? *J Am Coll Cardiol* 46:835–837, 2005
19. Sasso FC, Torella D, Carbonara O, Ellison GM, Torella M, Scardone M, Marra C, Nasti R, Marfella R, Cozzolino D, Indolfi C, Cotrufo M, Torella R, Salvatore T: Increased vascular endothelial growth factor expression but impaired vascular endothelial growth factor receptor signaling in the myocardium of type 2 diabetic patients with chronic coronary heart disease. *J Am Coll Cardiol* 46:827–834, 2005
20. Waltenberger J: Impaired collateral vessel development in diabetes: potential cellular mechanisms and therapeutic implications. *Cardiovasc Res* 49:554–560, 2001
21. Rees DA, Alcolado JC: Animal models of diabetes mellitus. *Diabet Med* 22:359–370, 2005
22. Petro AE, Cotter J, Cooper DA, Peters JC, Surwit SJ, Surwit RS: Fat, carbohydrate, and calories in the development of diabetes and obesity in the C57BL/6J mouse. *Metabolism* 53:454–457, 2004
23. Burcelin R, Crivelli V, Dacosta A, Roy-Tirelli A, Thorens B: Heterogeneous metabolic adaptation of C57BL/6J mice to high-fat diet. *Am J Physiol Endocrinol Metab* 282:E834–E842, 2002
24. Couffinhal T, Silver M, Zheng LP, Kearney M, Witzenbichler B, Isner JM: Mouse model of angiogenesis. *Am J Pathol* 152:1667–1679, 1998
25. Chou E, Suzuma I, Way KJ, Opland D, Clermont AC, Naruse K, Suzuma K, Bowling NL, Vlahos CJ, Aiello LP, King GL: Decreased cardiac expression of vascular endothelial growth factor and its receptors in insulin-resistant and diabetic States: a possible explanation for impaired collateral formation in cardiac tissue. *Circulation* 105:373–379, 2002
26. Dimmeler S, Zeiher AM: Akt takes center stage in angiogenesis signaling. *Circ Res* 86:4–5, 2000
27. Datta SR, Brunet A, Greenberg ME: Cellular survival: a play in three Akts. *Genes Dev* 13:2905–2927, 1999
28. Semenza GL: Regulation of hypoxia-induced angiogenesis: a chaperone escorts VEGF to the dance. *J Clin Invest* 108:39–40, 2001
29. Schiekofer S, Galasso G, Sato K, Kraus BJ, Walsh K: Impaired revascularization in a mouse model of type 2 diabetes is associated with dysregulation of a complex angiogenic-regulatory network. *Arterioscler Thromb Vasc Biol* 25:1603–1609, 2005
30. Leiter EH: Nonobese diabetic mice and the genetics of diabetes susceptibility. *Curr Diab Rep* 5:141–148, 2005
31. Shalaby F, Rossant J, Yamaguchi TP, Gertsenstein M, Wu X-F, Breitman ML, Schuh AC: Failure of blood-island formation and vasculogenesis in Flk-1-deficient mice. *Nature* 376:62–66, 1995
32. Fong G-H, Rossant J, Gertsenstein M, Breitman ML: Role of the flt-1 receptor tyrosine kinase in regulating the assembly of vascular endothelium. *Nature* 376:66–70, 1995
33. Zeng H, Dvorak HF, Mukhopadhyay D: Vascular permeability factor (VPF)/vascular endothelial growth factor (VEGF) receptor-1 down-modulates VPF/VEGF receptor-2-mediated endothelial cell proliferation, but not migration, through phosphatidylinositol 3-kinase-dependent pathways. *J Biol Chem* 276:26969–26979, 2001
34. Bussolati B, Dunk C, Grohman M, Kontos CD, Mason J, Ahmed A: Vascular endothelial growth factor receptor-1 modulates vascular endothelial growth factor-mediated angiogenesis via nitric oxide. *Am J Pathol* 159: 993–1008, 2001